Lasers in Manufacturing Conference 2023

Melt pool detection in closed loop control for Laser-Directed Energy Deposition wire processing

David Brinkmeier[a,*], Steffen Boley[a], Alexander Peter[a], Volkher Onuseit[a], Tobias Menold[a], Thomas Graf[a], Andreas Michalowski[a]

[a]*Institut für Strahlwerkzeuge (IFSW), University of Stuttgart, Pfaffenwaldring 43, 70569 Stuttgart, Germany*

Abstract

Melt pool detection in wire-based laser metal deposition is essential for ensuring the quality and efficiency of the additive manufacturing process. One of the most common methods for detecting the melt pool is through the use of high-speed cameras. Our coaxial imaging setup captures images of the melt pool at a high resolution, which are then processed in real time on the programmable logic controller of the processing station. These techniques include image segmentation, thresholding, and edge detection to identify the boundaries of the melt pool and extract various parameters such as size, shape and position. In particular the width and length of the melt pool are then used for process control, such as adjusting the laser power, wire feed rate and other parameters. The use of these techniques allows for real-time monitoring and control of the deposition process, leading to improved product quality and increased efficiency.

Keywords: L-DED Wire; closed loop control; process control; image processing

1. Introduction

Laser metal deposition with wire is an innovative technology in the field of 3D printing for the production of components made of various metals. In contrast to other additive laser processes, the advantage is that the metal semi-finished product is fed in wire form. This makes the process significantly cheaper and easier to handle than powder-based processes.

However, this rather novel and complex process does not yet have the necessary process stability and consistent quality. For example, starting and stopping the printing process, temperature and surface

* Corresponding author. Tel.: +49-711-685-69747
E-mail address: david.brinkmeier@ifsw.uni-stuttgart.de.

fluctuations, as well as geometry-dependent uncontrolled flow of the molten bath, lead to process instabilities that are difficult to predict. A review of the literature reveals a daunting list of possible process anomalies in Directed Energy Deposition (DED) processes (Michael Liu et al., 2021), illustrating the predicament of controlling the machining process with open-loop techniques: A high degree of reliability cannot be achieved with the established path planning methods, as the complex interaction between the molten pool and its environment cannot be calculated in advance with a reasonable amount of effort.

In order to increase the robustness and ease of use of the machining process, the idea is to use using self-learning feedback controllers based on different sensors inputs. The control architecture provides for three central parameters and objectives, two of which are currently implemented. In the final state, all parameters are to be controlled simultaneously. The objectives are:

1) Height control through a variable wire feed rate.
2) Temperature control through a variable irradiated laser power.
3) Wall thickness control through a variable focal plane of the laser spot.

The details of the control architecture and height control can be found in the accompanying publication Boley et al., 2023 and Becker et al., 2021. The wall thickness control will be the subject of a future publication.
This paper discusses the details and feasibility of temperature control based on a low-cost camera with sensitivity in the visible spectrum. Besides the price, a regular camera is additionally advantageous for adjustment purposes and is also able to provide information about the geometry of the melt pool in contrast to (1D) pyrometer-based solutions. Akbari and Kovacevic, 2019 and Baraldo et al., 2020 have shown this approach is viable, as it is generally expected image brightness correlates with melt pool temperature, but evaluation speed in these works is fairly slow and system integration hindered by previous technical bottlenecks.
Previous solutions were often implemented with asynchronous offline evaluation, i.e. fed as sensor variables into the cyclic logic of an industrial control system at random intervals and with random delays, which can lead to unpredictable behavior and does not allow consideration of the current state of the processing station within the (image) processing pipeline.
While temperature control for some DED processes is commercially available as fully integrated but proprietary solutions (SCIAKY Inc.) or as stand-alone systems based on MWIR thermal imaging technology (New Infrared Technologies) connected to a processing station via analog signals, these are either specialized solutions or fully integrated parts of a processing station and their evaluation logic may not be adaptable to the specific problem at hand.

2. Setup and image processing

The details of the optical path and the hardware infrastructure of the processing station are outlined in Fig. 1.

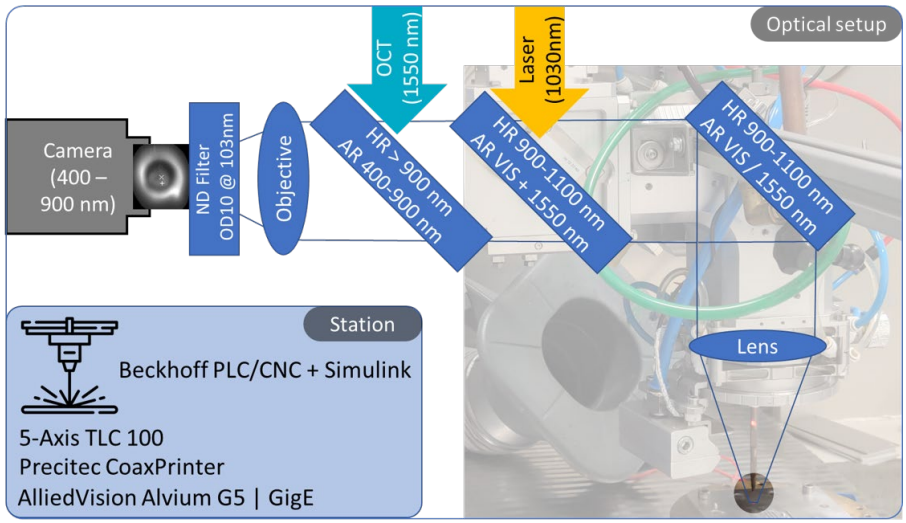

Fig. 1. Optical layout and processing station.

The camera shown schematically in the picture observes the machining process coaxially and is directly integrated into the Beckhoff programmable logic controller (PLC), which is required to enable real-time process control. As can be seen from the optical layout, the wavelength range that can be detected by the camera is limited to 400-900nm. Independently of this, in addition to the existing optics, additional optical filters were used to ensure that the laser wavelength of 1030nm is attenuated, so that corruption of the camera image by the processing laser is ruled out.

The image processing pipeline implemented on the PLC is shown in Fig. 2. Image evaluation was realized using TwinCat Vision, which essentially provides high-level access to a subset of functions loosely based on the open source image processing library OpenCV within the real-time environment of the industrial controller. This has also the advantage that the current state of the machine, for example the current axis coordinates or movement of the machining head relative to the workpiece, can be directly considered for the image evaluation.

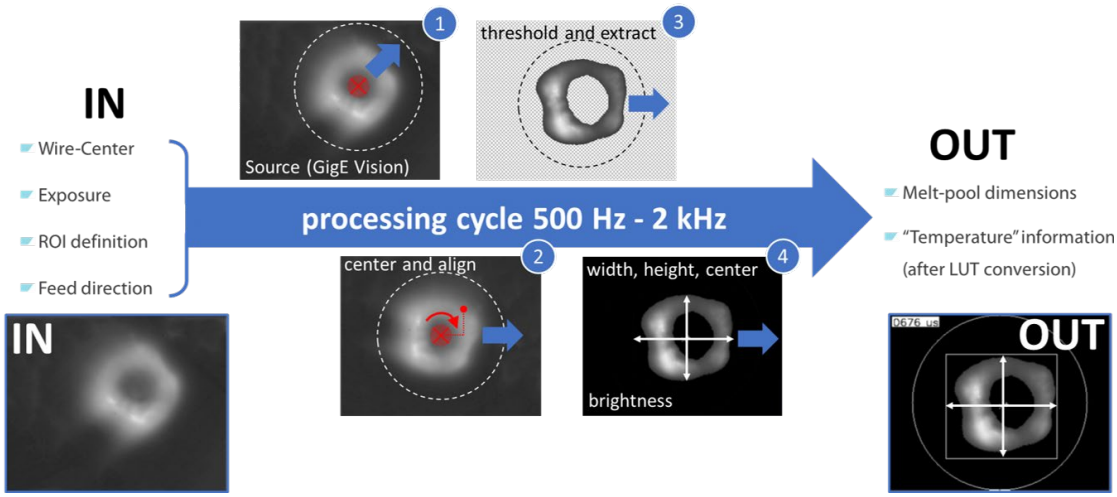

Fig. 2. Image processing pipeline. (1) The source image is centered based on the user-specified position of the wire center of gravity, creating a "blind spot" in the center of the melt pool as the wire is fed coaxially with the optical path. (2) The image is rotated based on the current axis movement of the processing station, ensuring that the vertical extent of the image always correlates to the melt pool width and the horizontal extent correlates to the melt pool length. (3) Thresholding based on the current image statistics is used to extract the melt pool. (4) Width, center and height are determined with a constant runtime evaluation (1460 µs +/- 33.2 µs per image in the current configuration) based on the centered image moments. Since the center of gravity of the molten bath should be static with respect to the user-defined center of gravity of the wire, this metric is used to filter data corrupted by asymmetric effects such as spatter. The average brightness (intensity) of the image is converted via a lookup table into an (uncalibrated) "temperature" value, which is used as input signal for the temperature sensor.

In principle, it can be expected that the brightness of the image correlates with the thermal emission of the molten bath. Considering the limited detectable wavelength spectrum, the spectral responsivity of the camera chip and the expected melt pool temperatures for metals, it can be further shown that the detected intensity is sufficiently well reproduced by the Stefan-Boltzmann law, i.e. the detected image intensity is approximately proportional to the fourth power of the melt pool temperature.

The conversion is done in the image processing pipeline by converting the image using a precalculated lookup table (LUT). The output is not calibrated, but it is expected that the result can be used as a measurand "temperature" as sensor input of the temperature controller, provided that the exposure time is constant (or by an appropriate correction if the exposure time is variable).

The term "temperature" is used in the following for this value, although this is of course only an assumption at this point and no calibration has taken place.

3. Experiments

Three representative tests were carried out with AlMg5 wire with a diameter of 1 mm. In all cases, the target geometry is hollow cylinders with a diameter of 75 mm. The processing parameters (or permitted parameter ranges) of the open-loop process (A), the bead height-controlled process (B) and the bead height as well as temperature-controlled process (C) are listed in Table 1.

Table 1. Processing parameters (or permitted parameter ranges for closed-loop processes).

Experiment	A	B	C
(Annular) Beam diameter	3 mm	3 mm	3 mm
Axis velocity	2m/min	2m/min	2m/min
(Goal) Layer height	0.5 mm	0.5 mm °C	0.5 mm
Process duration	12 minutes	12 minutes	12 minutes
Irradiated laser power	3 kW	3 kW	2-3.5 kW
Wire feed rate	4 m/min	0-6 m/min	0-6 m/min

The samples produced are shown in Fig. 3.

Fig. 3. Result with constant parameters (A), sample produced with variable wire feed rate (B), sample produced with variable wire feed rate and variable irradiated laser power (C).

As can be seen, sample A with constant process parameters has significant geometry errors. What cannot be seen is the fact that process A actually had to be manually restarted several times due to process instabilities. In contrast, the differences between the sample with height controller (B) and height controller and temperature controller (C) are not immediately obvious on a macroscopic level.

Based on the measurement data generated during the processes, the feasibility of the temperature control based on the VIS camera and subsequent image evaluation is discussed below.

4. Results

For an initial plausibility check of the temperature control, the average temperature and the average irradiated laser power are shown in Fig. 4 for the uncontrolled and controlled machining processes. As can be seen, both benchmark processes (A,B) without temperature control are comparatively too cold at the beginning of the machining process and too warm towards the end of the machining process when compared to the temperature-controlled machining process.

As can be seen in Fig. 4 (right), in the case of process (C), the temperature control initially increases the irradiated laser power, i.e. on the first layers close to the build platform, and drops with increasing component height or process duration to a value of about 2500W starting from 3000W.

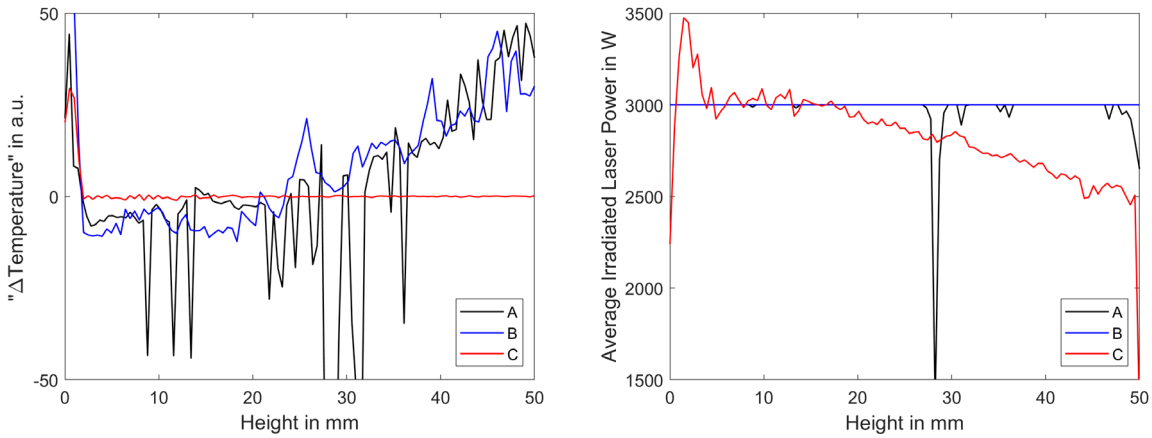

Fig. 4. Normalized average “temperature” per revolution determined through image processing (left) and corresponding average irradiated laser power (right). The horizontal axis (current work piece height) corresponds to the processing duration, which is roughly 12 minutes at the final height of 50 mm, as provided in Table 1. The temperature values are displayed as a deviation from the target value of the closed-loop process, meaning that a value of zero indicates a successful closed-loop process, negative values indicate a process colder than intended and positive values temperatures hotter than intended. The erroneous appearing signal in the case of attempt A is a consequence of the instability of the open-loop process and the necessity of the manual restarts of the machining process.

The trend shown in Fig. 4 thus intuitively indicates a plausible behavior for temperature control: In the vicinity of the build platform, a higher average laser power is required in accordance with the strong temperature gradients and the good heat dissipation, while towards the end of the machining process the heat dissipation from the high hollow cylinder into the substrate volume takes place more and more slowly and thus a lower laser power is required for a comparable machining process.

A central motivation for controlled for Laser-Directed Energy Deposition wire processing mentioned in the introduction is the control of inherent process instabilities and direction dependency. In order to illustrate these local dynamics, Fig. 5 shows the measured temperature data of the unrolled lateral surface of the cylinders in false colors plotted against the component height as y-axis.

The uniform color distribution in the case of experiment C, Fig. 5 (right), suggests a uniform temperature for the entire machining process at every point along the cylinder. In contrast, a strong and comparable directional dependence is evident in the case of processes A and B.

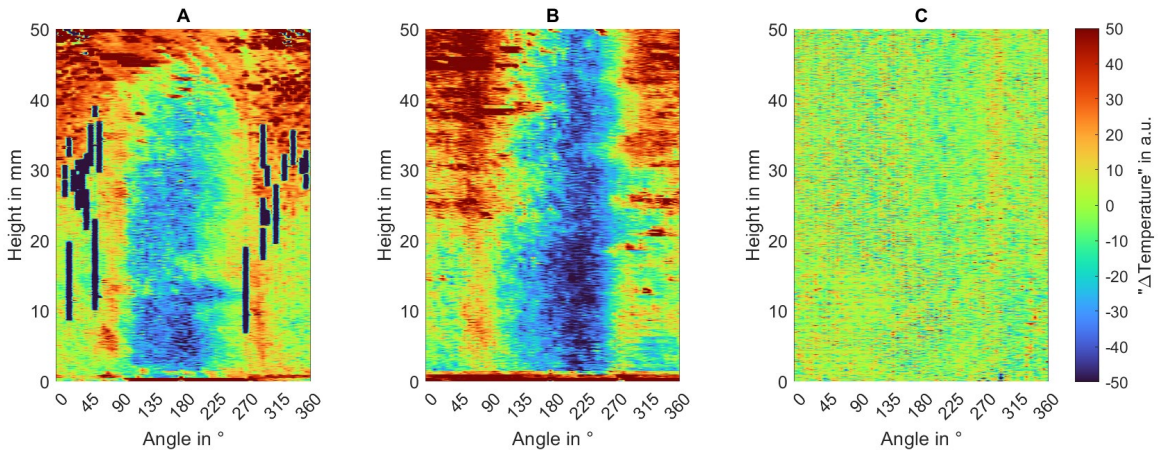

Fig. 5. From left to right: Unrolled lateral surface of the cylinders of process A (left), B (middle) and C (right). The vertical axis shows the component height, which also corresponds to the time axis. The horizontal axis describes the measurement data along the circumference of the cylinders, where here 0° shows the right side in the cylinders shown in Fig. 3, 90° at the top, 180° at the left and 270° at the bottom. The false color representation here, as in Fig. 4 (right), shows the "temperature" deviation determined from the image processing. The erroneous appearing signal in the case of attempt A is again consequence of the instability of the open loop process without bead height control.

The systematic of the directional dependence can be additionally confirmed by comparing the temperature distribution of the open-loop process, Fig. 6 (left), with the variation of the irradiated laser power of the controlled process, Fig. 6 (right). As can be seen, the irradiated laser power in the controlled process is higher exactly where the uncontrolled process is inherently colder and vice versa.

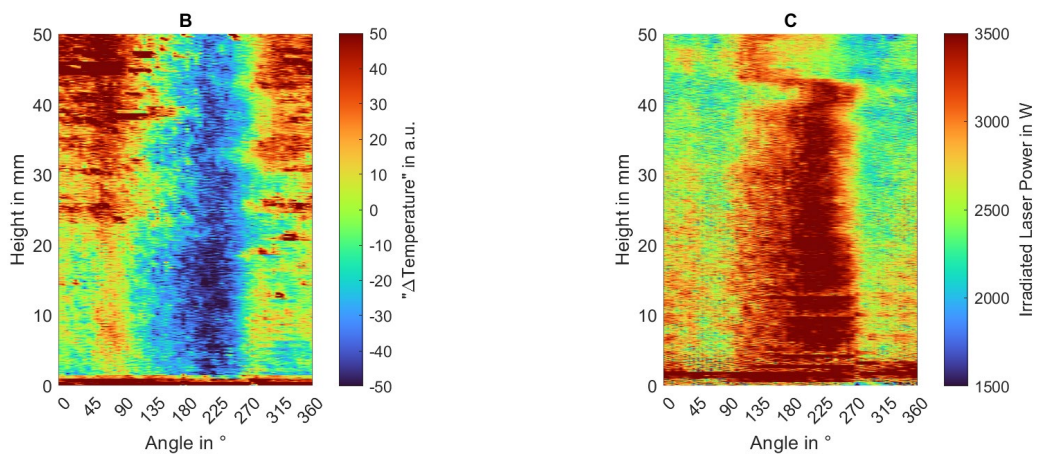

Fig. 6. Measured temperature distribution of experiment (B) with constant irradiated laser power over the circumference of the component (left) and variation of the irradiated laser power over the circumference of the component (C) with active temperature control.

Although the melt pool geometry or melt pool width is not yet used as a measured process variable of a bead coating width control loop at the present time, the existing data can be compared by way of example with data from the cross sections of the experiment series.

For this purpose, cross sections of the samples were created for measurement through direction 0° and 180°, based on the assumption that inhomogeneities in the wall thickness are also to be expected in the uncontrolled processes due to the significant temperature variations (according to our measurement) along these directions (see Fig. 5 and Fig. 6). An overview of the bead width measurements based on microscopy images is shown in Fig. 7.

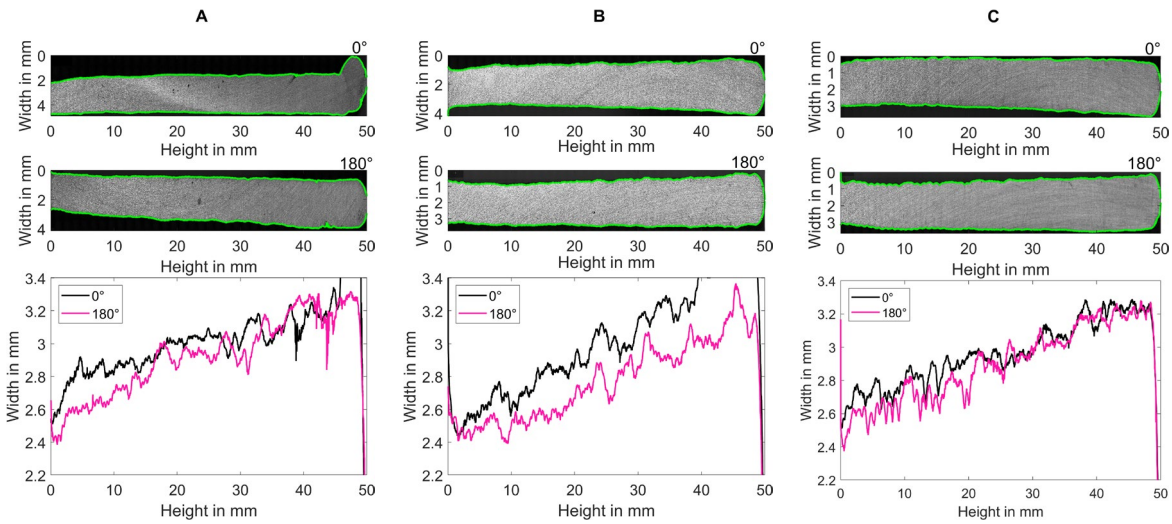

Fig. 7. Microscopy images of cross sections (top) and extracted bead widths (bottom) for experiment A through C from left to right.

In Fig. 7 it can be seen that the bead width increases in all experiments starting from the build platform upwards. The variation of the build width seems to be the smallest in the temperature-controlled process in agreement with the previous assumption.

The bead widths extracted via image evaluation is compared with the width measured from the cross sections in Fig. 8. The results show a good correlation with the measured widths.

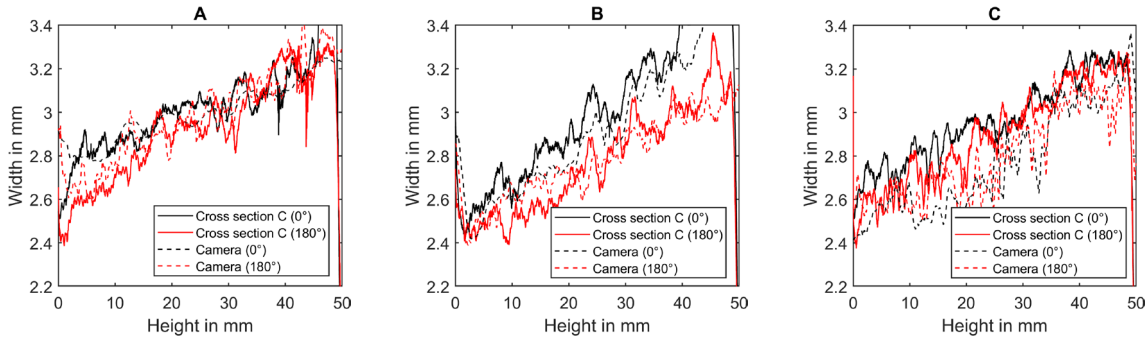

Fig. 8. Comparison of measured bead widths and bead widths determined via online image processing for experiment A through C from left to right.

5. Discussion

The results presented in chapter 4 are plausible insofar as we consider it confirmed that the temperature measurement and power control based on the visible wavelength range camera works reliably. The machining process is stabilized by the combined height and temperature control and, correlating with this, also seems to result in more uniform wall thicknesses of the overall component over the circumference.

Although the entire experimental setup of processing head with annular intensity distribution and coaxial wire feed as well as rotationally symmetrical (cylindrical) component is in principle designed to exhibit a low directional dependence, the results strikingly demonstrate the need for intelligent process control for the L-DED wire process. Regardless of where the asymmetric effects actually result from (e.g. from an incorrect laser-wire alignment or direction-dependent shielding gas supply and suction), the results make it clear that these problems can be controlled by an appropriate control system.

Furthermore, the (necessary) strong parameter variations generated by the control loop shows an a-priori unintuitive methodology for a process engineer, which is why we see ourselves affirmed conceptually in the fact that this laser machining process requires a high degree of automation and that an open-loop process based on conventional process development is not target-oriented.

Looking ahead, the agreement between the extracted melt pool widths and the measured wall thicknesses shows that a wall thickness control based on the determined image parameters should be possible. This topic will be evaluated in a future publication.

The implemented image processing pipeline and control architecture works well for the process shown, but it was already apparent in the raw data that the simultaneously running control loops for height and temperature control exhibit at least weak coupling, which could lead to instabilities of the control loops due to mutual influence, especially in the case of a future additional wall thickness control. In order to be able to map the complexity of these relationships, feature extraction based on machine learning approaches (in particular through neural and convolutional neural networks) is also being considered, since the inference of these models can now also be implemented within the real-time architecture of the industrial controller.

6. Conclusion

Our image processing and control architecture with combined height and temperature control leads to improved quality and process stability. The realization of the temperature control on the basis of an inexpensive camera with sensitivity in the visible wavelength range as well as the image processing pipeline

implemented directly on the industrial controller enables evaluation speeds beyond 500 Hz with constant evaluation time in the current configuration, as is necessary in an industrial controller to ensure that cycle time violations are avoided.

The strong directionality of the process, although the overall setup and experimental design would not suggest this, explicitly shows the need for an intelligent system architecture for the L-DED wire process.

As the last building block on the way to first-time-right, we believe that the additional control of the bead width, which is currently being implemented, can potentially transform this machining process from a fringe application to a laser machining process that is easily controllable and widely used in practice.

Acknowledgements

We would like to thank the Ministry of Science, Research and the Arts of the State of Baden-Württemberg for the financial support of the *InnovationCampus Future Mobility (ICM)*.

References

Akbari, Meysam; Kovacevic, Radovan (2019): Closed loop control of melt pool width in robotized laser powder–directed energy deposition process. In: *Int J Adv Manuf Technol* 104 (5-8), p. 2887–2898. DOI: 10.1007/s00170-019-04195-y.

Baraldo, Stefano; Vandone, Ambra; Valente, Anna; Carpanzano, Emanuele (2020): Closed-Loop Control by Laser Power Modulation in Direct Energy Deposition Additive Manufacturing. In: Lihui Wang, Vidosav Majstorovic, Dimitri Mourtzis, Emanuele Carpanzano, Govanni Moroni und Luigi Maria Galantucci (Hg.): Proceedings of 5th International Conference on the Industry 4.0 Model for Advanced Manufacturing. AMP 2020. 1st ed. 2020. Cham: Springer International Publishing; Imprint Springer (Lecture Notes in Mechanical Engineering), p. 129–143.

Becker, Dina; Boley, Steffen; Eisseler, Rocco; Stehle, Thomas; Möhring, Hans-Christian; Onuseit, Volkher et al. (2021): Influence of a closed-loop controlled laser metal wire deposition process of S Al 5356 on the quality of manufactured parts before and after subsequent machining. In: *Prod. Eng. Res. Devel.* 15 (3-4), p. 489–507. DOI: 10.1007/s11740-021-01030-w.

Boley, Steffen; Brinkmeier, David; Peter, Alexander; Onuseit, Volkher; Menold, Tobias; Graf, Thomas; Michalowski, Andreas (2023): Closed Loop Process Control for L-DED Wire 5-axis Processing. In: *Proc. Lasers in Manufacturing (LiM), Germany*.

Michael Liu; Abhishek Kumar; Satish Bukkapatnam; Mathew Kuttolamadom (2021): A Review of the Anomalies in Directed Energy Deposition (DED) Processes & Potential Solutions - Part Quality & Defects. In: *Procedia Manufacturing* 53, p. 507–518. DOI: 10.1016/j.promfg.2021.06.093.

New Infrared Technologies: CLAMIR. online available at https://www.clamir.com/en/, last checked on 23.06.2023.

SCIAKY Inc., IRISS: IRISS Interlayer Realtime Imaging & Sensing System. online available at https://www.sciaky.com/additive-manufacturing/iriss-closed-loop-control, last checked on 23.06.2023.